

UDK 53.086; 666.3.019; 622.785

Microstructure and Phase Composition of the Two-Phase Ceramic Synthesized from Titanium Oxide and Zinc Oxide

Galina M. Zeer^{1*)}, Elena G. Zelenkova¹, Natalia S. Nikolaeva¹, Sergey M. Zharkov^{1,2}, Artur K. Abkaryan¹, Anatoly A. Mikheev³

¹ Siberian Federal University, Krasnoyarsk, 660041, Russia

² Kirensky Institute of Physics, Federal Research Center KSC SB RAS, Krasnoyarsk, 660036, Russia

³ Siberian State Aerospace University, Krasnoyarsk, 660014, Russia

Abstract:

We have made investigations of the phase formation and microstructure on the ceramics obtained from a starting nanopowder mixture with the weight ratio $ZnO : TiO_2 = 4 : 1$. Ceramic is obtained at different sintering temperatures, namely, 948, 1223 and 1473 K. Using the characterization methods of electron microscopy, energy dispersive microanalysis and X-ray diffraction phase analysis it has been shown that the ceramics structure is consisted of two dispersed phases of Zn_2TiO_4 and ZnO with the grain sizes being in range 0,5-1 μm . It has been found also that, at ceramic's sintering temperature of 1223 K, the solid phase interactions are completed with the structure $ZnO : Zn_2TiO_4 \approx 1 : 1,5$ phase ratio.

Keywords: Nanopowders; Titanium oxide; Zinc oxide; Solid phase reaction; Ceramic.

1. Introduction

Nanostructures based on zinc and titanium oxides attract attention due to their peculiar structural, optical, optoelectronic and other characteristics. Zinc oxide, as a result of solid phase reactions in the process, for instance, can form by thermal annealing compounds of the spinel type in the form of tertiary oxides $ZnM^{[3+]}_2O_4$ or $Zn_2M^{[4+]}O_4$ with various metals such as Al, Cr, Fe, Ga, In, Sn, Sb, Ti, Mn, V [1-3]. Compounds based on ZnO-TiO₂ (zinc titanates) are technologically important since they possess specific properties hardly obtained using solely ZnO. In the ZnO-TiO₂ system six chemical compounds of various types are formed, where ortho- and metatitanate are the best studied [4-6]. Zinc orthotitanate Zn_2TiO_4 occurs in the form of crystals having cubic regular octahedra structure with the lattice parameter being $a = 0,846$ nm. The obtained compounds of zinc orthotitanate are found to be stable to temperature changes. Zinc metatitanate $ZnTiO_3$ occurs as hexagonal system crystals – ilmenite with the lattice parameters being $a = 0,508$ nm and $c = 1,392$ nm.

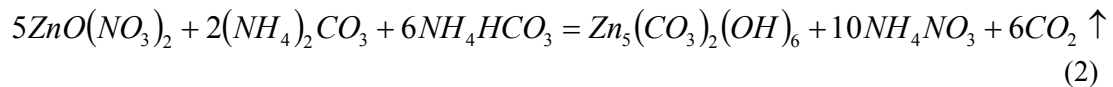
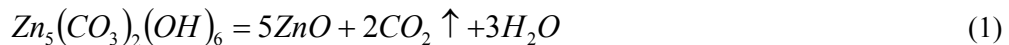
Zinc titanates are widely applied both as materials for radio electronic devices, photoelectrochemical cells, catalysts and gas sensors, as well as pigments, regenerated catalysts and absorbents for eliminating sulphur in related compounds at high temperatures [7-10]. Thus, great attention is being paid to the investigations of the titanate synthesis [9, 11-14].

*) Corresponding author: g-zeer@mail.ru

One of the practical applications of titanium oxide and zinc oxide is a possibility of their use as arc-quenching agents or dispersive hardening additives in electrical contact materials [15, 16]. Electrical contact materials have to possess such properties as durability and the ability to quench arcs which appear in the processes of contact closing and opening [17, 18]. As arc-quenching additives different oxides are usually used where metals are Zn, Mn, Cu, Sb, Ti, Pb, etc. [17-21]. According to our assumption, zinc titanate in combination with zinc oxide can also serve as a dispersive hardening phase in copper electrical contact materials. Hardness, durability and lifetime of the items can be increased in such a manner if we compare it to the materials presently used [15,16]. Upon sintering of an electrical contact material a composite is obtained whose copper matrix includes zinc oxide and zinc titanate formed in the process of a solid-phase reaction of titanium oxide and zinc oxide. This work is aimed at investigating the phase formation, microstructure and properties of the two phase ceramics ZnO/Zn₂TiO₄, obtained at different sintering temperatures.

2. Experimental Procedure

To produce investigated ceramic samples ZnO and TiO₂ nanopowders were used. Zinc oxide was obtained by the thermal decomposition of zinc hydroxide carbonate, reaction (1). Zinc hydroxide carbonate was synthesized by mixing aqueous solutions of ammonium hydrocarbonate and zinc nitrate, reaction (2):



The TiO₂ nanopowder was obtained by the method of conductor electric explosion. During ultrasonical agglomerate grinding ZnO and TiO₂ nanopowders were mixed in the ethanol medium and mixture was homogenized. After drying at T= 353 K in order to improve interparticle friction and pressing characteristics the obtained powder mixture was granulated by introducing a 3% solution of polyvinyl butyral in ethanol as a plasticizer into the mixture. The samples were then pressed in a compression mould at a $P \leq 150$ MPa pressure. To investigate the density, microstructure and elemental composition of the particular phases the following samples were derived: (1) green bodies, compacts; (2) sintered specimens in different temperature regimes.

The microstructure, phase and elemental composition of the nanopowders were studied by the methods of transmission electron microscopy (TEM) and electron diffraction using JEOL JEM-2100. The microstructure and elemental composition of the phases in the sintered ceramics were investigated by scanning electron microscopy (SEM) using JEOL JSM-7001F equipped with an energy dispersive X-ray spectrometer (Oxford Instruments). The X-ray diffraction phase analysis of the compacts was performed on the X-ray diffractometer BRUKER D8 ADVANCE under dynamic heating in air, with the platinum carrier. Heating was performed from 298 K to 1223 K at a rate of 10 K/min with isothermal exposure for 30 min at 873 K, 1073 K and 1223 K. Synchronous TGA/DSC thermal analysis of the ZnO and TiO₂ nanopowders was carried out using NETZSCH STA 449 C Jupiter, with the heating rate 10 K/min.

3. Results and Discussion

Two phases – zinc oxide ZnO and zinc titanate Zn₂TiO₄– are suggested to be used as dispersive hardening and arc-quenching components in the structure of the electrical contact

material. The main arc-quenching component is zinc oxide, thus, presumably, the optimal phase ratio is $\text{ZnO} : \text{Zn}_2\text{TiO}_4 \approx 1 : 1,5$. To obtain the given optimal phase ratio in the sintered ceramics, according to the phase diagram of ZnO-TiO_2 [22] an starting oxide nanopowder mixture was prepared with the oxides weight ratio equal to $\text{ZnO} : \text{TiO}_2 = 4 : 1$.

The shape and sizes of the initial nanopowders were determined by the method of transmission electron microscopy. The investigation of the ZnO powder by high resolution transmission electron microscopy shows that the particles have a shape close to a sphere with the average radial size equal to 8 ± 2 nm (Fig. 1,a). The particles have a defectless crystalline structure. The electron diffraction pattern obtained by nanodiffraction from a single particle of ZnO, is seen to be a single crystal (inset Fig.1,a).

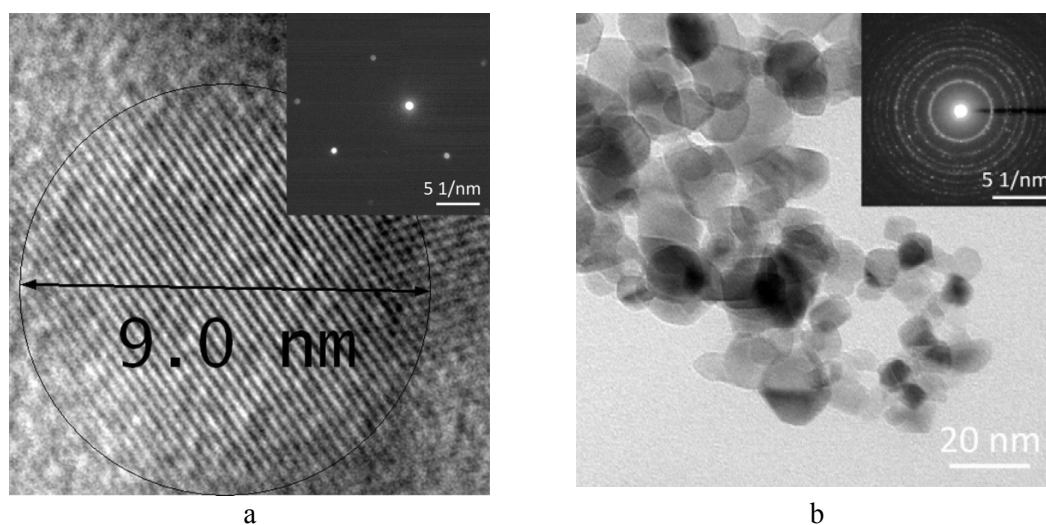


Fig. 1. TEM images of the nanopowders in the initial state: a – ZnO; b – TiO_2 (the insets show the electron diffraction patterns).

The interpretation of the electron diffraction patterns obtained by selected area electron diffraction from a group of particles as well as by nanodiffraction from single particles shows that the observed diffraction reflections correspond to the phase ZnO with the hexagonal structure, the space group being $P6_3mc$ with the lattice parameters declared as $a=0,325$ nm, $c=0,521$ nm (PDF 4+ card #00-036-1451). The investigations of the titanium oxide powder shows the particles to have the average size of 15 ± 5 nm (Fig. 1,b). The analysis of the selected area electron diffraction pattern (see the inset in Fig. 1,b) obtained from a group of particles shows the diffraction reflections to correspond to the anatase TiO_2 phase with the tetragonal structure, and the space group $I4_1/amd$ with the lattice parameters declared as $a=b=0,387$ nm, $c=0,962$ nm (PDF 4+ card #04-011-0664).

The process of phase formation during solid phase reaction in the ZnO-TiO_2 system was studied using X-ray diffraction analysis of the phase composition in the dynamic heating mode with isothermal exposure of the nanopowder mixture of ZnO and TiO_2 . Fig. 2 presents X-ray diffraction patterns acquired after isothermal exposure at temperatures at which should occur solid phase interactions in the ZnO-TiO_2 system. As it can be seen from the X-ray diffraction pattern, at $T=298$ K the phase composition of the sample corresponds to the initial oxide mixture but the reflections corresponding to the oxides are slightly broadened. This can be subscribed to the small sizes of the initial powder particles. At $T=873$ K the increase of the intensity and the decrease of the width of the diffraction reflections are observed in the initial components. This is due to grain coarsening during sintering. The result of the solid phase reaction between ZnO and TiO_2 do not become detectable in the X-ray diffraction pattern until isothermal exposure at $T=1073$ K. The entire TiO_2 interacts with zinc oxide, forming

zinc meta- (ZnTiO_3) and ortho- (Zn_2TiO_4) titanate. Further temperature increase results in the ZnTiO_3 phase disappearing and after exposing the sample to $T = 1223$ K, only two phases are detected: ZnO and Zn_2TiO_4 . This phase composition corresponds to the area of the ZnO-TiO_2 phase diagram [22] at the nanopowder ratio $\text{ZnO} : \text{TiO}_2 = 4 : 1$. Thus, $T = 1223$ K is sufficient for completing the phase formation and sintering of the ceramics with the desired composition.

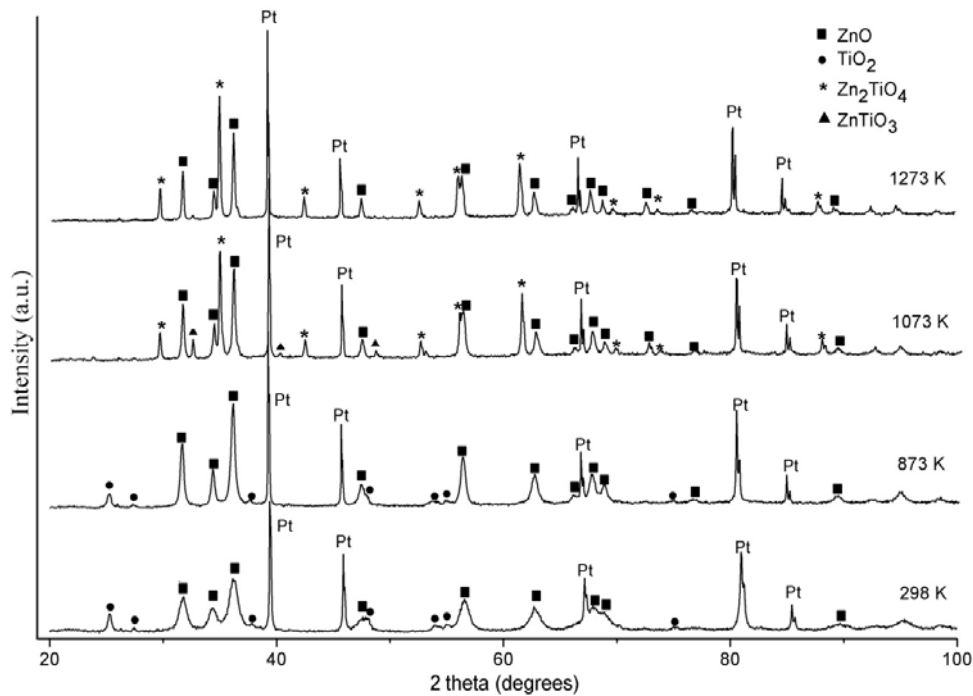
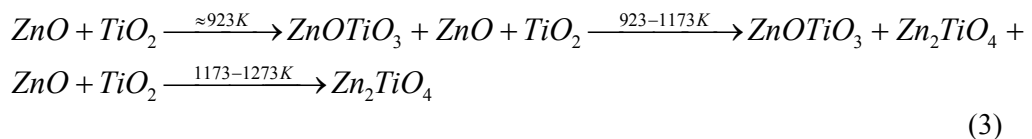


Fig. 2. X-ray patterns acquired at different temperatures of sintering of the ZnO-TiO_2 nanopowder mixture.

To determine the transformations occurring in the process of heating the ZnO-TiO_2 nanopowder mixture, thermogravimetric coupled with differential scanning (TG/DSC) thermal analysis were performed (Fig.3). The total mass loss recorded on the thermogravimetric curve was equal to $\sim 7\%$, which is due to the sample dehydration and the plasticizer burnt out. In the range of 873-1273 K the differential scanning calorimetry curve has a complicated profile. The thermal effects are not accompanied by the mass variations, what evidences the solid phase reactions and sintering events in the system.

The combination of thermal effects in this temperature range at the given $\text{ZnO}:\text{TiO}_2$ ratio can be described by the following series of reactions:



Thus, the results obtained by X-ray diffraction phase analysis and thermo gravimetric analyses correlate mutually each other and are consistent with the ZnO-TiO_2 phase diagram.

To study the phase formation during the solid state reaction upon sintering of the ZnO and TiO_2 nanopowders mixture, compacts and sintered specimens were obtained and their microstructure and elemental composition of the present phases were investigated. Compacts, named as batch 1, were sintered at 948 K, which is slightly higher temperature than solid state

reaction onset temperature of zinc meta-titanate formation. Reaction started from titanium oxide and zinc oxide reactants (Fig. 2). The temperature of 1223 K produced compacts, named as batch 2. This temperature corresponds to the sintering temperature for electrical contact materials based on copper powder with the average particle size of 20-40 μm . The ceramic's sintering temperature equal to 1473 K for the investigated starting composition produced sintered specimens, named batch 3.

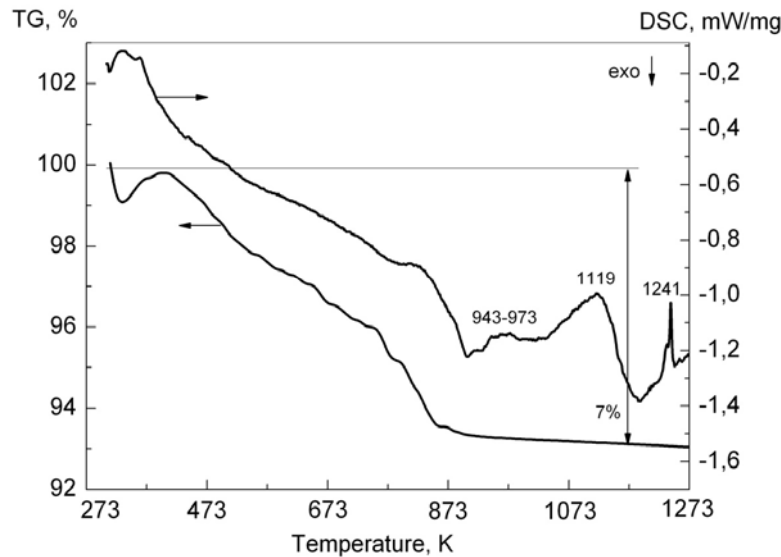


Fig. 3. TG-, DSC- curves for heating the TiO_2 -ZnO nanopowder mixture.

The density of the compacts was determined by the geometrical method, for the sintered specimens it was determined by the hydrostatical method. The porosity was calculated on the basis of the density. In the case of the compacts we deal with open porosity and in the case of the sintered specimens we estimate closed porosity. The density and porosity of the compacts and sintered specimens are presented in Fig. 4, with the used value of theoretical density for calculations equal to $\rho_{\text{theory}} = 5.15 \text{ g/cm}^3$. The relative porosity decreased by 5 %, what resulted from sintering at 948 K.

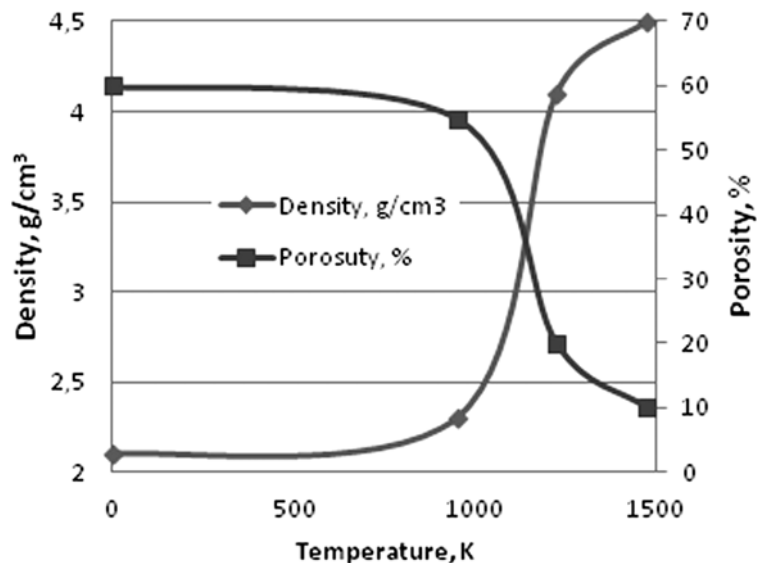


Fig. 4. The dependence of the ceramic density and porosity on the sintering temperature.

Microstructure analysis of the specimens allowed us to determine the initial stage of the contact between the nanopowder particles as a neck formation in the agglomerates (Fig. 5, a). At the sintering temperature of 1223 K the ceramic density increased almost two times respectively, with rigid contacts formed between the already formed grains with their size being estimated in 0,1-0,7 μm interval (Fig. 5, b). The porosity is rather high $\approx 20\%$, with the pore size determined from the SEM images being 0,1-1 μm , thus, the temperature of isothermal sintering (1223 K) is considered insufficient for the sintering completion with this particular starting oxides composition.

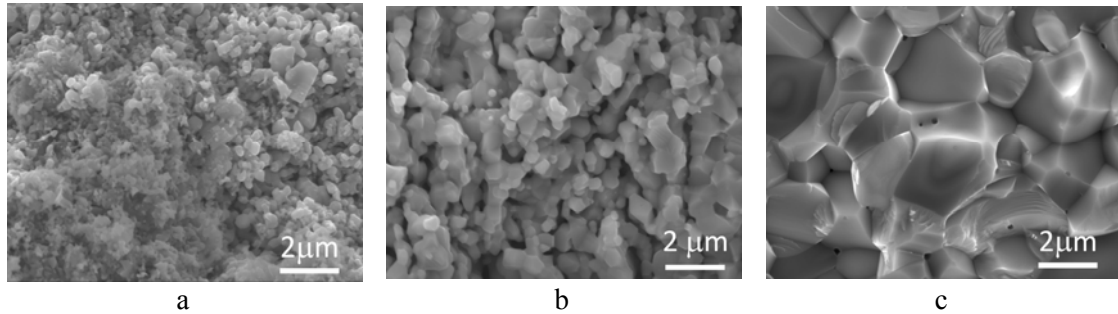


Fig. 5. SEM images of the surface destruction of the ceramics sintered at different temperatures: a – 948 K; b – 1223 K; c – 1473 K

Sintering at 1473 K resulted in the pore size reduction to the average size of 0,1 μm followed by a relative porosity reduction to 8%. However, the presence of recrystallization is noteworthy which results in a significant coarsening of the grains which diameter rise up to 5 μm . Consequently, this led to the decrease of the ceramic's strength (Fig. 5,c).

The microstructure of polished surfaces of the sintered ceramics was studied by SEM using composition contrast technique (Fig. 6, a-c) allowing us to distinguish phases in gradations of gray. This enabled us to subscribe phases with heavier elements to a darker gray undertone, while phase with lighter elements is subscribed to brighter undertone. The elemental composition of the ceramics phases was determined by the method of energy dispersive microanalysis and the markers of characteristic EDS spectra are denoted in the microstructure images (Fig. 6,a-c). The results are presented in Tab. I.

Tab. I The elemental composition of the sample ceramics sintered at different temperatures

№ spect rum	Elemental composition of the EDS spectrum (at.%)								
	$T_{\text{sint.}} = 948 \text{ K}$			$T_{\text{sint.}} = 1223 \text{ K}$			$T_{\text{sint.}} = 1473 \text{ K}$		
	O	Ti	Zn	O	Ti	Zn	O	Ti	Zn
1	54.08	-	45.92	44.51	-	55.49	48.96	-	51.04
2	58.27	16.46	25.27	60.55	10.38	29.07	57.06	13.93	29.01
3	65.77	34.23	-	-	-	-	-	-	-

In the SEM image of the microstructure sample (Fig. 6, a) sintered at $T = 948 \text{ K}$ one can see dark-gray grains, with titanium and oxygen revealed in their composition (Tab. I, spectrum №1) and darker-gray grains consisting of zinc and oxygen, which is almost completely consistent with the composition of the initial powders ZnO and TiO₂ (Tab. I, spectrum №2). According to the evidence of characteristic EDS spectra № 1, 2 (Fig. 5,a; 6,a), the solid phase interaction between ZnO and TiO₂ at $T_{\text{sint.}} = 948 \text{ K}$ is at initial stage.

The analysis of the microstructure images (Fig. 5,b; 6,b) and composition of the characteristic EDS spectra (Tab. I) acquired for the ceramics sintered at 1223 K, reveals that two-phase ceramics is formed, and the process of the solid-phase reaction in the ZnO–TiO₂

system is completed, which is evidenced by the results of the energy dispersive analysis (Tab. I). At 1473 K sintering continues accompanied by the grain coarsening (Fig. 5,c; 6,c).

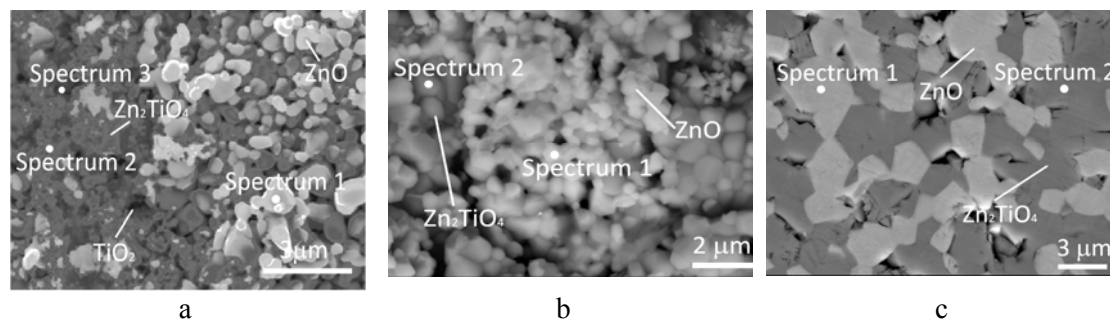


Fig. 6. SEM images of the polished surfaces of the ceramics sintered at temperatures: a – 948 K; b – 1223 K; c – 1473 K

Characteristic EDS spectra № 1 (Tab.I) acquired for the light-gray crystallites (see Fig. 6,b,c) of the ceramics sintered at 1223 K and 1473 K, show the presence of zinc and oxygen in the ratio which nearly corresponds to ZnO. Characteristic EDS spectra № 2 (Tab. I) show the elemental composition of the dark-gray crystallites (see Fig. 6,b,c) where zinc, titanium and oxygen are present, which approximately corresponds to zinc titanate – Zn_2TiO_4 . The microstructure study of the ceramics sintered at 1223 K and 1473 K shows that the volumetric ratio of the phases has the following relation $ZnO : Zn_2TiO_4 \approx 1 : 1,5$.

4. Conclusion

Observed two phase ceramics were obtained by solid phase sintering of the nanopowder mixture of ZnO and TiO_2 (weight ratio being 4 : 1). The sintering temperatures were equal to – 948, 1223 and 1473 K. The dependence of the compact density and porosity on the sintering temperature was studied. Energy dispersive analysis and SEM revealed that the obtained two phase ceramic has the following phase ratio – $ZnO : Zn_2TiO_4 \approx 1 : 1,5$. The initial stage of sintering is found to be at 948 K and it is declared with forming neck contacts between dispersed powder particles inside the nanopowder agglomerates. The grained structure is found to form at sintering temperature of 1223 K, with the size of the formed Zn_2TiO_4 and ZnO phases in a 0,5 to 1 μm range and the sample having an increased, rather high density. The results of the X-ray phase analysis show that the solid phase reactions in the ZnO / TiO_2 system are completed at $T_{sint.} = 1223$ K with the formation of the two-phase ceramics ZnO / Zn_2TiO_4 . The coarsening of the structure is found to occur at the sintering temperature of 1473 K, with the grain size increased up to range between 2 and 5 μm .

Acknowledgments

This work is supported by the Russian Foundation for Basic Research, grant no. 16-08-00789 a.

5. References

1. Z. L. Wang, Novel Nanostructures of ZnO for Nanoscale Photonics, Optoelectronics, Piezoelectricity, and Sensing, Appl. Phys. A., 88, (2007) 7–15.

2. H. J. Fan, Y. Yang, and M. Zacharias, ZnO-Based Ternary Compound Nanotubes and Nanowires, *J. Mater. Chem.*, 19, (2009) 885–900.
3. H. J. Fan, M. Knez, R. Scholz, K. Nielsch, E. Pippel, D. Hesse, M. Zacharias and Gösele, U, Monocrystalline Spinel Nanotube Fabrication Based on the Kirkendall Effect, *Nat. Mater.*, 5, (2006) 627–631.
4. H. T. Kim, Y. Kim, M. Valant, and D. Suvorov, Titanium Incorporation in Zn_2TiO_4 Spinel Ceramics, *J. Am. Ceram. Soc.*, 84 [5], (2001) 1081–1086.
5. M.R. Mohammadi, and D.J. Fray, Low Temperature Nanostructured Zinc Titanate by an Aqueous Particulate Sol-Gel Route: Optimisation of heat Treatment Condition Based on Zn:Ti Molar Ratio, *J. Eur. Ceram. Soc.*, 30, (2010) 947–961.
6. E. Hosono, S. Fujihara, M. Onuki, and T. Kimura, Low-Temperature Synthesis of Nanocrystalline Zinc Titanate Materials with High Specific Surface Area, *J. Am. Ceram. Soc.*, 87 [9], (2004) 1785–1788.
7. Y.-S. Chang, Y.-H. Chang, I.-G. Chen, G.-J. Chen, Y.-L. Chai, Synthesis and Characterization of Zinc Titanate Nano-crystal Powders by Sol-Gel Technique, *J. Crystal Growth*, 243, (2002) 319–326.
8. Y.-S. Chang, Y.-H. Chang, I.-G. Chen, G.-J. Chen, Y.-L. Chai, T.-H. Fang, and S.Wu, Synthesis, Formation and Characterization of $ZnTiO_3$ Ceramics, *Ceram. Int.*, 30, (2004) 2183–2189.
9. N. Labus, Z. Z. Vasiljević, D. Vasiljević-Radović, S.Rakić, M. V. Nikolić, Two Step Sintering of $ZnTiO_3$ nanopowder, *Sci. Sinter.*, 49 (2017) 51-60.
10. N. Obradovic, N. Labus, T. Sreckovic, and S. Stevanovic, Reaction Sintering of the $2ZnO-TiO_2$ System, *Sci. Sinter.*, 39 [2], (2007) 127–132.
11. M.V. Nikolić, N. Obradović, K.M. Paraskevopoulos, T.T. Zorba, S.M. Savić, and M.M. Ristić, Far Infrared Reflectance of Sintered Zn_2TiO_4 , *J. Mater. Sci.*, 43, (2008) 5564–5568.
12. Y. Yang, X. W. Sun, B. K. Tay, J. X. Wang, Z. L. Dong, and H. M. Fan, Twinned Zn_2TiO_4 Spinel Nanowires Using ZnO Nanowires as a Template, *Adv. Mater.* 19 [14], (2007) 1839–1844.
13. M. Pineda, J. L. G. Fierro, J. M. Palacios, C. Cilleruelo, E. Garcia, and J. V. Ibarra, Characterization of Zinc Oxide and Zinc Ferrite Doped With Ti or Cu as Sorbents for Hot Gas Desulphurization, *Appl. Surf. Sci.*, 119 [1-2], (1997) 1–10.
14. D. Barreca, E. Comini, A. P. Ferrucci, A. Gasparotto, C. Maccato, C. Maragno, G. Sberveglieri, and E. Tondello, First Example of $ZnO-TiO_2$ Nanocomposites by Chemical Vapor Deposition: Structure, Morphology, Composition, and Gas Sensing Performances, *Chem. Mater.*, 19 [23], (2007) 5642–5649.
15. G. M. Zeer, E. G. Zelenkova, A. V. Sidorak, O. N. Ledyeva, and M. Yu. Kuchinskii, Microstructure and Properties of a Copper Electrocontact Material With a Nanodispersed Titanium Dioxide Additive, *Techn. Phys.*, 58 [5], (2013) 710–714.
16. G. M. Zeer, Investigation of the Microstructure and Properties of Electrocontact Silver–Zinc Oxide Nanopowder Material, *Phys. Met. Metall.*, 113 [9], (2012) 902–906.
17. M. Braunovic, V.V. Konchits, and N.K. Myshkin, *Electrical Contacts: Fundamentals, Applications, and Technology*. London, New York, CRC Press, Teilor and Francis Gtoup, 2007.
18. Holm H. *Electric Contacts*. Berlin, Springer-Verlang, 2010.
19. X. Wang, H. Yang, M. Chen, J. Zou, and S. Liang, Fabrication and Arc Erosion Behaviors of $AgTiB_2$ Contact Materials, *Powder Technol.*, 256, (2014) 20–24.

20. M. Chen, X. Wang, J. Zou, and S. Liang, Effect of Additives on Microstructure and Properties of Novel AgTiB₂ Composite, Rare Metal Mat. Eng., 41 [12], (2012) 2228–2232.
21. C.P. Wu, D.Q. Yi, J. Li, L.R. Xiao, B. Wang, and F. Zheng, Investigation on Microstructure and Performance of Ag/ZnO Contact Material, J. Alloy. Compd., 457 [1–2], (2008) 565–570.
22. F. H. Dulin, and D. E. Rase, Phase Equilibria in the System ZnO-TiO₂, J. Am. Ceram. Soc., 43 [3], (1960) 125–131.

Садржај: У раду смо истраживали фазни састав и микроструктуру керамика добијених из полазних нанопрахова, и то у односу $ZnO : TiO_2 = 4 : 1$. Керамика је добијена при различитим температурама синтеровања, 948, 1223 и 1473 К. Методе за карактеризацију као што су електронска микроскопија, дисперзивна микроанализа, и рендгенска дифракција су показале да у структуру керамике улазе две фазе Zn_2TiO_4 и ZnO са величином зрна између 0,5-1 μm . Када је температура синтеровања керамике 1223 К, завршена је реакција у чврстој фази при односу $ZnO : Zn_2TiO_4 \approx 1 : 1,5$.

Кључне речи: нано прахови; титан диоксид; цинк оксид; реакције у чврстом стању; керамика

© 2016 Authors. Published by the International Institute for the Science of Sintering. This article is an open access article distributed under the terms and conditions of the Creative Commons — Attribution 4.0 International license (<https://creativecommons.org/licenses/by/4.0/>).

